

Original Article

LncRNA NORAD promotes the progression of myocardial infarction by targeting the miR-22-3p/PTEN axis

Chunxia Li*, Lihui Zhang, Xingpeng Bu, Guofang Chu, Xiaofang Zhao, and Yaru Liu

Shanxi Bethune Hospital, Shanxi Academy of Medical Sciences, Tongji Shanxi Hospital, Third Hospital of Shanxi Medical University, Taiyuan 030032, China

*Correspondence address. Tel: +86-351-8368114; E-mail: ChunxiaLigrow@163.com

Received 12 August 2021 Accepted 11 November 2021

Abstract

NORAD is a newly identified long non-coding RNA (lncRNA) that plays an important role in cancers. NORAD has been found to be highly expressed in the mouse model of acute myocardial infarction (AMI). However, the role of NORAD in the regulation of AMI remains unknown. In the present study, we aimed to investigate the function of NORAD in AMI and explore the potential regulatory mechanisms. A mouse model of AMI was established and NORAD was knocked-down. The infarcted size of heart tissues and the cardiac function were evaluated. In addition, two cardiomyocyte cell lines were treated with hypoxia/re-oxygenation (H/R) to mimic AMI *in vitro*. Luciferase reporter assay, RNA pull-down assay, fluorescence *in situ* hybridization, qRT-PCR, and western blot analysis were performed. Apoptotic cells and the levels of L-lactate dehydrogenase (LDH) and malondialdehyde (MDA) were detected. Our results show that downregulation of NORAD efficiently attenuates heart damage in the AMI mouse model. NORAD interacts with miR-22-3p. Knock-down of NORAD inhibits H/R-induced cell apoptosis and reduces LDH and MDA levels, while its effects are abolished by miR-22-3p inhibitor. MiR-22-3p interacts with PTEN and inhibits its expression. Overexpression of miR-22-3p inhibits H/R-induced cell apoptosis and reduces LDH and MDA levels, while its effects are abolished by overexpression of PTEN. Finally, overexpression of NORAD inhibits the AKT/mTOR signaling pathway, and its effects are attenuated by overexpression of miR-22-3p. Taken together, our study reveals that NORAD promotes the progression of AMI by regulating the miR-22-3p/PTEN axis, and the AKT/mTOR signaling may also be involved in the regulatory processes.

Key words acute myocardial infarction, NORAD, miR-22-3p, PTEN, AKT/mTOR pathway

Introduction

Acute myocardial infarction (AMI), which happens due to the acute interruption of myocardial blood flow, is a common and potential life-threatening disease with an increasing incidence and high mortality [1,2]. Reperfusion therapy after AMI can effectively restore the blood supply and nutritional support in the ischemic myocardium and save the dying myocardium [3]. The pathogenesis of AMI has been identified to be associated with multiple factors, of which cardiomyocyte apoptosis is considered as the crucial component [4,5]. Understanding the molecular mechanisms involved in cardiomyocyte apoptosis is critical to develop novel and efficient molecular targets for AMI.

Long non-coding RNAs (lncRNAs), a class of regulatory RNAs lacking protein coding function and approximately 200 nucleotides in length, were previously considered as a type of transcriptional

noise, but nowadays have been identified as critical regulators in tumor development [6–9]. NORAD is a newly identified lncRNA that participates in the progression of a series of human cancers. For instance, NORAD is significantly upregulated in esophageal squamous cell carcinoma (ESCC) tissues [10]. NORAD can suppress the metastasis of lung and breast cancers through sequestering S100P, and the expression of NORAD is inhibited by the YAP pathway [11]. One previous study suggested that NORAD enhances the hypoxia-induced epithelial-mesenchymal transition (EMT) process to promote metastasis in pancreatic cancer [12]. Another study showed that NORAD promotes the progression of thyroid carcinoma by targeting miR-202-5p [13]. In addition, Yang *et al.* [14] revealed that NORAD could enhance the TGF- β pathway to promote the development of hepatocellular carcinoma through directly sponging miR-202-5p. NORAD was found to be highly expressed in the myocardial

infarction (MI) of left ventricle tissues in mice [15]. However, whether NORAD plays a role in MI remains unknown.

Increasing studies have revealed that the abnormal expression of microRNAs (miRNAs) is closely associated with biological processes such as neuroprotection and tumorigenesis [16]. MiR-22-3p is located on chromosome 17 (17p13.3). Studies have shown that miR-22-3p is involved in many diseases. For example, miR-22-3p can control the amyloid β deposit in the mice model of Alzheimer's disease [17]. MiR-22-3p can regulate the proliferation of retinoblastoma cells by targeting alpha-enolase 1 [18]. In addition, Chen *et al.* [19] revealed the mechanism of berberine treatment in hepatocellular carcinoma (HCC), specifically, berberine can upregulate the expression of miR-22-3p to inhibit the proliferation of HCC cells through targeting Sp1. Furthermore, miR-22-3p restrains the fibrogenesis of post-myocardial infarction in mice via targeting PTAFR [20]. However, the function of miR-22-3p in AMI remains unclear.

Phosphatase and tensin homolog (PTEN) was first identified as a tumor suppressor by regulating the cell division cycle and removing phosphate groups to modify proteins and fats [21,22]. Previous studies have demonstrated that the PTEN may trigger cardiomyocyte cells to undergo apoptosis and exacerbate myocardial dysfunction, and the inactivation of cardiac-specific PTEN can protect the heart against functional failure, fibrosis and MI in a mouse model [23,24]. In addition, PTEN was reported to be a negative regulator of AKT and a mammalian target of rapamycin (mTOR) signaling in multiple diseases [25,26]. In AMI, PTEN induces the apoptosis of cardiomyocyte cells possibly through modulating the PI3K/AKT signaling pathways [27,28], however the regulatory network of PTEN involved in cardiomyocyte apoptosis is unknown.

In the present study, we showed that NORAD could promote the development of AMI by targeting the miR-22-3p/PTEN axis, and the AKT/mTOR signaling might participate in the regulation of NORAD in AMI.

Materials and Methods

Animal model

C57BL/6 adult mice (male, approximately 4 weeks old) were purchased from Shanxi Bethune Hospital, Shanxi Academy of Medical Sciences (Taiyuan, China). Mice were kept at room temperature (approximately 22–26°C) with a 12/12-h light/dark cycle and 50%–70% humidity. A mouse model of AMI was established through the ligation of the left anterior descending coronary artery as previously described [29]. After ligation for 30 min, reperfusion was performed by cutting the knot in the ligature. For the Sham group, the procedure was the same but without transient artery ligation. All animal experiments were performed according to the Institutional Animal Ethics Guidelines for the Care and Use of Research Animals of Shanxi Bethune Hospital, Shanxi Academy of Medical Sciences. This study was approved by the Ethics Committee of Shanxi Bethune Hospital, Shanxi Academy of Medical Sciences. To explore the specific function of NORAD *in vivo*, approximately lentivirus carrying si-NORAD (silencing of NORAD) or negative control (si-NC) was intravenously injected into mice (10 mg/kg body weight) through the tail vein at 24 h before surgery. Mice were randomly divided into 4 groups (4 mice in each group): Sham + si-NC group, Sham + si-NORAD group, AMI + si-NC group and AMI + si-NORAD group.

Determination of MI

At 24 h after AMI or sham operation, mice were euthanized via the

intraperitoneal injection of avertin (2,2,2-tribromoethanol; Sigma-Aldrich, Darmstadt, Germany) (20 mg/kg). The whole hearts were cut into 2 mm thick slices and stained with 1% triphenyltetrazolium chloride (TTC) at 37°C for 20 min after washing out the remaining blood. The sizes of the TTC-stained area (red staining, ischemic but viable tissue) and unstained area (infarct myocardium, INF) were analyzed using the Image Pro Plus 6.0 software (Media Cybernetics Inc., Bethesda, USA).

Evaluation of cardiac function

The cardiac function of mice was evaluated by the motion-mode echocardiography under the VEVO 770 high-resolution *in vivo* imaging system (FUJIFILM VisualSonics Inc., Bothell, USA). The mean value of left ventricular fractional shortening (LVFS) was analyzed by M mode, and left ventricular internal dimensions (LVIDs) were evaluated at end-systole(s) through a four-chamber view.

HE staining assay

At the end of animal experiments, the hearts of mice were rapidly collected and washed twice with phosphate buffered saline (PBS), fixed with 4% paraformaldehyde, embedded in paraffin wax, and cut into 4 sections with 5 μ m in thickness. Then the sections (4 mice in each group) were stained with hematoxylin and eosin (H&E) as previously described [30]. Histological changes were observed under a light microscope (Olympus, Tokyo, Japan).

Cell culture

The mouse cardiomyocyte cell line HL-1 (cat. no. SCC065) and the mouse cardiomyocyte cell line AC16 (cat. no. SCC109) were obtained from Sigma-Aldrich. Cells were cultured in DMEM medium containing 10% FBS and 1% penicillin-streptomycin (Nacalai Tesque Inc., Tokyo, Japan) at 37°C with 5% CO₂. To establish the cell model with hypoxia/re-oxygenation (H/R), HL-1 cells were firstly kept in a hypoxia incubator (approximately 1% O₂, 5% CO₂, and 94% N₂) at the density of 5 \times 10⁵ cells/mL for 20 h. Then cells were incubated under the normoxic conditions for 4 h and collected for the subsequent experiments.

Cell transfection

Si-NORAD (silencing of NORAD), si-NC (control), miR-22-3p mimics (miR-22-3p overexpression) or miR-NC (control) were transfected into HL-1 cells using the Lipofectamine 2000 (Invitrogen, Carlsbad, USA) according the manufacturer's instructions. The sequences were as follows: si-NORAD forward: 5'-GCUGUCGGAAGAGAGAAUUTT-3', reverse: 5'-AUUUCUCUCUCCGACAGCTT-3'; si-NC forward: 5'-UUCUCCGAACGUGUCACGUTT-3', reverse: 5'-ACGUGACACGUUCGGAGAATT-3'; miR-22-3p mimics: 5'-GGCTGAGCCGAGTAGTTCTTTCAGTGGCAAGCTTTATGTCTGACCCAGCTAAAGCTGCCAGTTGAAGAACTGTTGCCCTCTGCC-3'; miR-22-3p inhibitor: 5'-CTCGCTTCGGCAGCAC-3'; and miR-NC: 5'-UUCUCCGAACGUGUCACGUTT-3'. MiR-22-3p inhibitor was purchased from GenePharma (Shanghai, China). For the overexpression of NORAD, the cDNA fragment of NORAD was amplified and cloned into the expression vector pcDNA3.1 (Richmond, Canada). The concentration of si-NORAD/si-NC was 500 ng/well and miR-22-3p inhibitor/mimic/miR-NC was approximately 100 nM. After transfection for 48 h, cells were collected for the subsequent experiments.

Luciferase reporter assay

The cDNA fragment of NORAD/PTEN containing either the pre-

dicted potential miR-22-3p binding site (wild-type, WT) or mutant (MUT) sequence were amplified by PCR and cloned into *Renilla* luciferase reporter vector pmirGLO (Promega, Madison, USA). HL-1 cells were transfected with luciferase reporter plasmids and miR-22-3p mimics or miR-NC. After transfection for 48 h, cells were plated, and the relative luciferase activity was evaluated using a dual-luciferase reporter system (Promega).

Fluorescence *in situ* hybridization (FISH)

FISH was performed according to the reference. Briefly, HL-1 cells were grown on the culture dish, washed with cold PBS for 3 times, and then fixed in 4% paraformaldehyde. Then, HL-1 cells were incubated with prehybridization buffer at 40°C for 4 h, followed by incubation with NORAD-FITC (GenePharma) at 37°C for 30 min, miR-22-3p-mCherry (GenePharma) for 30 min and DAPI (Beyotime Biotechnology, Shanghai, China) for 10 min after washing. The images were captured using a confocal microscope.

Quantitative real-time polymerase chain reaction (qRT-PCR)

Total RNAs of heart tissues of mice or cultured cells were extracted using Trizol reagent (Invitrogen, Carlsbad, USA). qRT-PCR reactions were prepared using the SYBR Green PCR kit (Toyobo, Shanghai, China) and PCR was performed on the 7500 Fast Real-time PCR system (Applied Biosystems, Foster City, USA). The relative fold changes were calculated using the $2^{-\Delta\Delta Ct}$ method [31] with β -actin and U6 as the internal references. The primers used in this study were as follows: miR-22-3p forward: 5'-GCTGAGCCGCGAGTAGTTCTT-3', reverse: 5'-GGCAGAGGGCAACAGTTCTT-3'; PTEN forward: 5'-TAGAGCGTGCGGATAATGAC-3', reverse: 5'-GATGCTCCTCTACTGTTTT-3'; β -actin forward: 5'-CCTCTATGCCAACACAGTGC-3', reverse: 5'-CATCGTACTCCTGCTTGCTG-3'; and U6 forward: 5'-CTCGCTTCGGCAGCAC-3', reverse: 5'-AACGCTTCACGAATTTGCG-3'.

Western blot analysis

Total proteins of cultured cells were isolated using RIPA lysis buffer. Approximately equal amount of protein samples was separated by 10% SDS-PAGE and then transferred into PVDF membranes (Immobilon-P; Millipore, Billerica, USA). After being blocked with 5% skim milk, the membranes were incubated with primary antibodies including anti-PTEN (1:1000; Abcam, Cambridge, UK), anti-AKT (1:2000; CST, Beverly, USA), anti-p-AKT (1:1000; CST), anti-mTOR (1:2000; Abcam), anti-p-mTOR (1:1000; Abcam), and anti- β -actin (1:2000; Abcam) at 4°C overnight. After 3 times wash, the membranes were incubated with HRP-conjugated secondary antibody at room temperature for 2–3 h. Finally, the protein bands were visualized using ECL reagent, and the images of bands were captured and analyzed using the ImageJ2X software.

RNA pull-down assay

HL-1 cells were transfected with biotin-labeled negative control, biotin-labeled miR-22-3p WT or biotin-labeled miR-22-3p MUT. The probes used were as follows: miR-22-3p WT: 5'-UGUCAAGAA-GUUGACCGUCGAA-3'; and miR-22-3p MUT: 5'-UGUCAAGGA-GUUCAAACAGCGA-3'. After transfection for 48 h, the whole-cell extract was incubated with M-280 streptavidin magnetic beads (Invitrogen) at 4°C for 3–5 h. The co-precipitated RNA was purified using Trizol reagent supplemented with proteinase K (Invitrogen)

and analyzed by qRT-PCR.

Detection of L-lactate dehydrogenase (LDH) and malondialdehyde (MDA)

The LDH level and MDA levels in cell supernatant were detected using the LDH assay kit (ab102526; Abcam) or Cellular Malondialdehyde Test kit (A003-2; Nanjing Jiancheng Bioengineering Institute, Nanjing, China) following the manufacturer's instructions.

Flow cytometry

Cells were harvested at 48 h post-transfection and re-suspended in pre-cooled PBS. Next, 5 μ L of Annexin V-FITC solution (Sangon Biotech, Shanghai, China) was added and incubated at room temperature in the dark for 15 min. After centrifugation and washing with binding buffer, cells were re-suspended in a solution containing 190 μ L binding buffer and 10 μ L propidium iodide (PI; Sangon Biotech). Then cell apoptosis was detected by flow cytometry on a Beckman flow cytometer (Beckman Coulter, Fullerton, USA).

Statistical analysis

Data were presented as the mean \pm standard deviation (SD) from at least 3 independent experiments. Differences between two groups were determined by Student's *t*-test. Differences among multiple groups were determined using one-way ANOVA followed by a post hoc Tukey's test. $P < 0.05$ was considered to be statistically significant.

Results

Downregulation of NORAD inhibits AMI progression *in vivo*

To explore the function of NORAD in AMI, the mouse model with AMI was established and NORAD was knocked-down. qRT-PCR results showed that si-NORAD significantly decreased the expression level of NORAD in both Sham group ($P < 0.001$) and AMI group ($P < 0.001$; Figure 1A). Then the effects of NORAD in AMI-induced mice were evaluated. TTC staining assay results showed that knockdown of NORAD significantly decreased the infarction size of mice compared with si-NC control in the AMI group ($P < 0.001$; Figure 1B), while it had no effect on the infarction size of mice in the Sham group (Figure 1C). Mouse echocardiography indicated that downregulation of NORAD increased the LVFS and decreased the LVIDs compared with si-NC control in the AMI group, while it had no effect on LVFS or LVIDs in the Sham group ($P < 0.05$; Figure 1D, E, G). In addition, HE staining showed that there was a normal histoarchitecture in the Sham group, while an obvious necrosis of myofibers with cell infiltration was observed in the AMI group (Figure 1F). Meanwhile, knockdown of NORAD significantly ameliorated these damages compared with si-NC control in the AMI group. In addition, we also found that NORAD was upregulated in blood samples of AMI patients using the GEO database (Figure 1H). These results indicated that downregulation of NORAD could efficiently attenuate AMI-induced heart damage.

NORAD acts as a sponge of miR-22-3p

To explore the specific mechanism of NORAD in AMI, HL-1 cells were treated with H/R to establish an *in vitro* MI model. qRT-PCR results showed that the expression level of NORAD was sig-

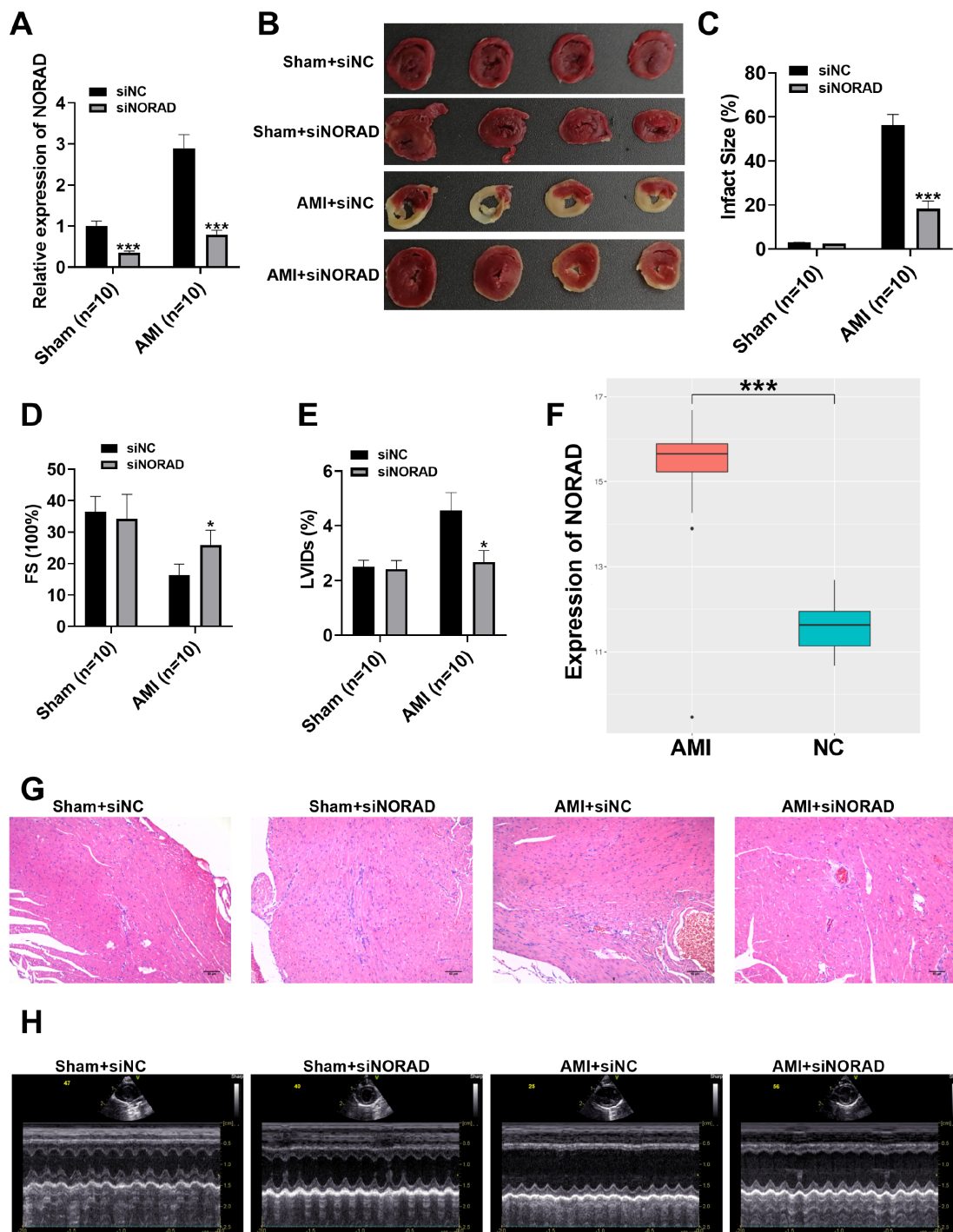


Figure 1. Silencing of NORAD attenuates AMI progression *in vivo* Mice were injected with si-NORAD or si-NC, and then subject to AMI induction. (A) The mRNA level of NORAD in heart tissues was evaluated by qRT-PCR. (B) The infarcted size of heart tissues sections was analyzed by using TTC staining. (C) Quantitative analysis of the infarcted area. The cardiac functions of mice including LVFS (D) and LVIDs (E) were evaluated. (F) Histopathological examination of cardiac function by HE staining assay, and representative AMI injury areas were indicated with white boxes. Scale bar = 5 mm. (G) Typical images of echocardiography. (H) The expression level of NORAD of blood samples from normal people and AMI patients ($n=4$) with GEO database. * $P < 0.05$, *** $P < 0.001$. LVFS: left ventricular fractional shortening; LVID: left ventricular internal dimension.

nificantly increased in H/R-stimulated cells compared with those in cells treated with normal conditions ($P < 0.001$; Figure 2A). Starbase v2.0 predicted that miR-22-3p is a potential target of NORAD (Figure 2B). Therefore, miR-22-3p mimics were transfected into HL-1 cells and the transfection efficiency was confirmed by qRT-PCR (Figure

2C). Next, luciferase reporter assay was performed to confirm the relationship between NORAD and miR-22-3p, and the results showed that miR-22-2p mimics significantly reduced the relative luciferase activity of WT NORAD vector compared with NC mimics ($P < 0.001$), while it had no effect on the luciferase activity in the

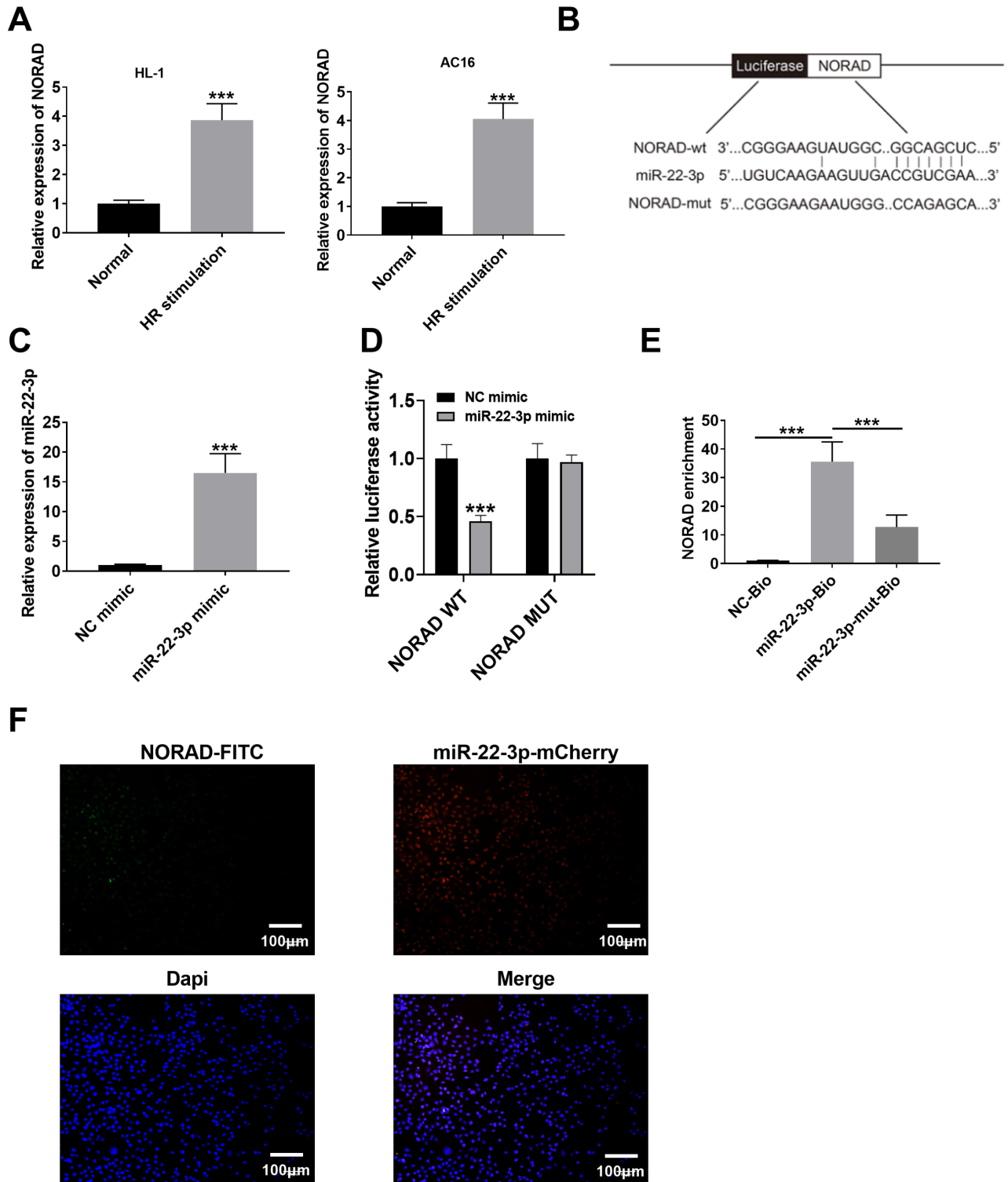


Figure 2. NORAD acts as a sponge of miR-22-3p (A) HL-1 and AC16 cell lines were treated with or without H/R stimulation, and the mRNA level of NORAD was evaluated by qRT-PCR. (B) The putative binding site between NORAD and miR-22-3p was predicted by Starbase v2.0. (C) HL-1 cells were transfected with miR-22-3p mimics or miR-NC control, and the transfection efficiency was confirmed by qRT-PCR. (D) HL-1 cells were co-transfected with luciferase reporter plasmids containing WT or MUT NORAD and miR-22-3p mimics or NS mimics, and the relative luciferase activity was evaluated by a dual-luciferase reporter system. (E) RNA pull-down assay was performed using biotin-labeled miR-22-3p WT or biotin-labeled miR-22-3p MUT, and the enrichment fold of NORAD was analyzed by qRT-PCR. (F) FISH assay was used to examine the expression and location of NORAD and miR-22-3p in HL-1 cells. Scale bar = 100 µm. * $P < 0.05$, ** $P < 0.01$, *** $P < 0.001$.

cells transfected with MUT NORAD vector (Figure 2D). In addition, RNA pull-down assay showed that NORAD was significantly enriched in biotin-labeled miR-22-3p WT group compared with that in the biotin-labeled miR-22-3p MUT group ($P < 0.001$; Figure 2E). Finally, FISH assay was performed to examine the expression and location of NORAD and miR-22-3p in HL-1 cells. The results showed that NORAD and miR-22-3p were mainly expressed in the nuclei (Figure 2F). These results indicated that NORAD might act as a sponge of miR-22-3p.

MiR-22-3p inhibitor reverses si-NORAD-induced inhibitory effect on the apoptosis of H/R-treated HL-1 cells

To further determine the negative correlation between NORAD and

miR-22-3p, HL-1 and AC16 cells were transfected with si-NORAD, OE-NORAD (overexpression of NORAD) or their corresponding negative controls. qRT-PCR results showed that si-NORAD significantly increased the expression level of miR-22-3p compared with si-NC ($P < 0.001$), while OE-NORAD decreased the expression level of miR-22-3p compared with negative control (empty vector pcDNA3.1) ($P < 0.001$; Figure 3A). Meanwhile, the levels of LDH and MDA in the cultured supernatant of H/R-treated HL-1 cells were evaluated. The results showed that si-NORAD significantly decreased the LDH level compared with negative control ($P < 0.01$), while co-transfection with si-NORAD and miR-22-3p inhibitor reversed si-NORAD-induced inhibitory effect on LDH release ($P < 0.01$; Figure 3B). Meanwhile, si-NORAD significantly decreased the MDA level compared with negative control ($P < 0.01$), and miR-

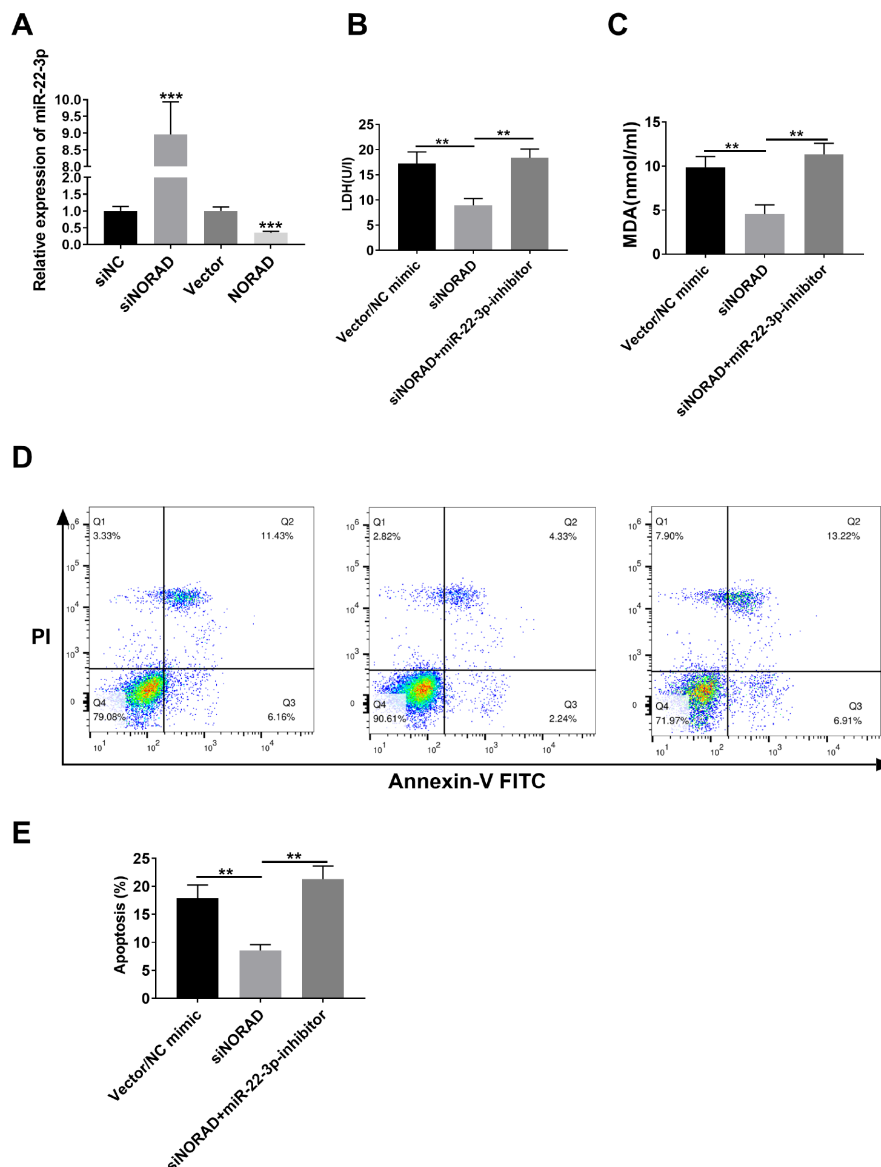


Figure 3. Silencing NORAD inhibits the apoptosis of H/R-treated HL-1 cells through sponging miR-22-3p (A) HL-1 cells were transfected with si-NORAD, OE-NORAD (NORAD overexpressing vector), or corresponding negative controls (si-NC and the empty vector pcDNA3.1), and then treated with H/R. The mRNA level of miR-22-3p was evaluated by qRT-PCR. HL-1 cells were transfected with si-NORAD or co-transfected with si-NORAD and miR-22-3p inhibitor and then treated with H/R. The LDH release (B) and MDA level (C) in the cell supernatants were evaluated using the corresponding detection kits. (D,E) Cell apoptosis was evaluated by flow cytometry. ** $P < 0.01$, *** $P < 0.001$.

22-3p inhibitor reversed the si-NORAD-induced inhibitory effect ($P < 0.01$; Figure 3C). In addition, flow cytometric analysis revealed that si-NORAD significantly inhibited H/R-induced cell apoptosis, while its effect was attenuated by miR-22-3p inhibitor ($P < 0.01$; Figure 3D,E). These data suggested that downregulation of NORAD significantly inhibited the apoptosis of H/R-treated HL-1 cells by down-regulating miR-22-3p.

PTEN is a target of miR-22-3p

To further investigate the molecular mechanisms of miR-22-3p in AMI, Targetscan was used to predict the potential targets of miR-22-3p. It showed that miR-22-3p potentially binds to the 3'-untranslated region (3'-UTR) of PTEN (Figure 4A). Therefore, PTEN was over-expressed by the transfection of OE-PTEN (PTEN overexpressing vector) or the empty vector pcDNA3.1, and qRT-PCR results showed that OE-PTEN significantly increased the expression level of

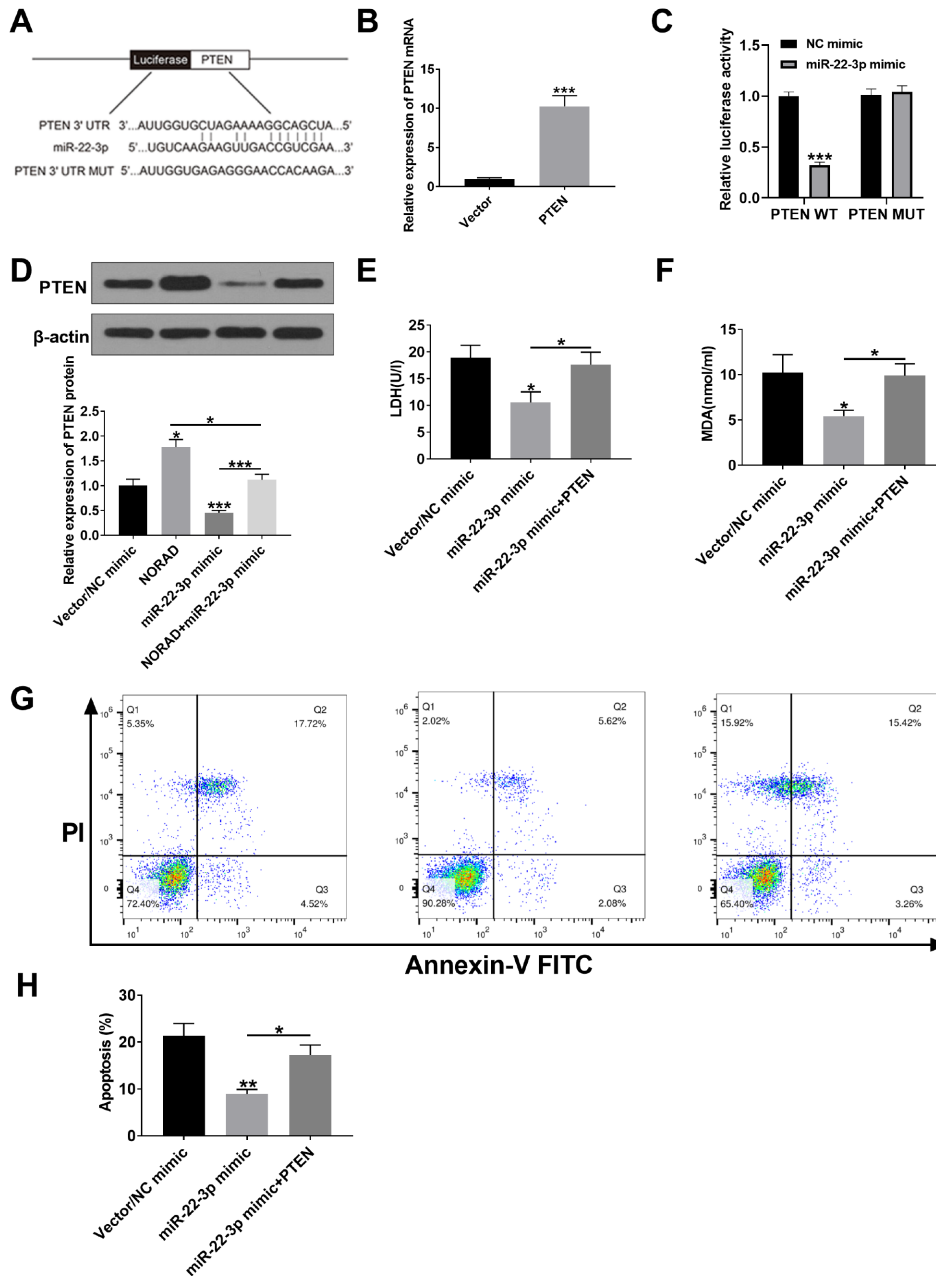


Figure 4. PTEN is a target of miR-22-3p (A) The putative interaction between miR-22-3p and PTEN was predicted by Targetscan. (B) HL-1 cells were transfected with OE-PTEN (PTEN overexpressing vector) or empty vector pcDNA3.1, and then treated with H/R. The mRNA level of PTEN was evaluated by qRT-PCR. (C) HL-1 cells were co-transfected with recombinant luciferase reporter plasmids and miR-22-3p mimics or NC mimics, and the relative luciferase activity was evaluated by a dual-luciferase reporter system. (D) HL-1 cells were transfected with OE-NORAD, miR-22-3p, or co-transfected with OE-NORAD and miR-22-3p, then treated with H/R. The protein expression level of PTEN was evaluated by western blot analysis. (E-H) HL-1 cells were transfected with miR-22-3p mimics or co-transfected with miR-22-3p mimics and OE-PTEN, and then treated with H/R. The LDH release (E) and MDA level (F) in the cell supernatants were evaluated using the corresponding detection kits. (G,H) Cell apoptosis was evaluated by flow cytometry. * $P < 0.05$, ** $P < 0.01$, *** $P < 0.001$.

PTEN compared with the empty vector control ($P < 0.001$; Figure 4B). To confirm their interaction, luciferase reporter assay was performed, and the results showed that miR-22-3p mimics significantly decreased the relative luciferase activity of 3'-UTR WT PTEN compared with that of miR-NC control ($P < 0.001$), while it had no effect on the luciferase activity in cells transfected with 3'-UTR MUT PTEN (Figure 4C). Meanwhile, overexpression of NORAD increased the expression level of PTEN protein, and miR-22-3p mimics decreased the expression level of PTEN protein and attenuated OE-NORAD-induced up-regulation of PTEN ($P < 0.05$; Figure 4D). Furthermore, miR-22-3p mimics significantly decreased the levels of LDH and MDA compared with the negative control ($P < 0.05$), while overexpression of PTEN reversed miR-22-3p mimics-mediated inhibitory effect on the LDH release and MDA expression ($P < 0.05$; Figure 4E,F). In addition, miR-22-3p mimics significantly decreased the apoptosis of H/R-treated HL-1 cells ($P < 0.01$), while its effect on apoptosis was attenuated by OE-PTEN

($P < 0.05$; Figure 4G,H). These results suggested that overexpression of miR-22-3p could inhibit the apoptosis of H/R-treated HL-1 cells by targeting PTEN.

Upregulation of NORAD inhibits the mTOR/AKT signaling pathway by regulating miR-22-3p

Finally, the impact of NORAD on the mTOR/AKT signaling was investigated. HL-1 cells were transfected with OE-NORAD and (or) miR-22-3p mimics, and then treated with H/R. The expression levels of PTEN, AKT, p-AKT, mTOR, and p-mTOR were detected by western blot analysis (Figure 5A). The results showed that overexpression of NORAD significantly decreased the expression levels of p-AKT ($P < 0.05$) and p-mTOR ($P < 0.001$) compared with the negative control, while miR-22-3p mimics increased the expression levels of p-AKT ($P < 0.05$) and p-mTOR and attenuated the effects of NORAD on p-AKT and p-mTOR (Figure 5B). These results suggested that upregulation of NORAD could significantly inhibit the activa-

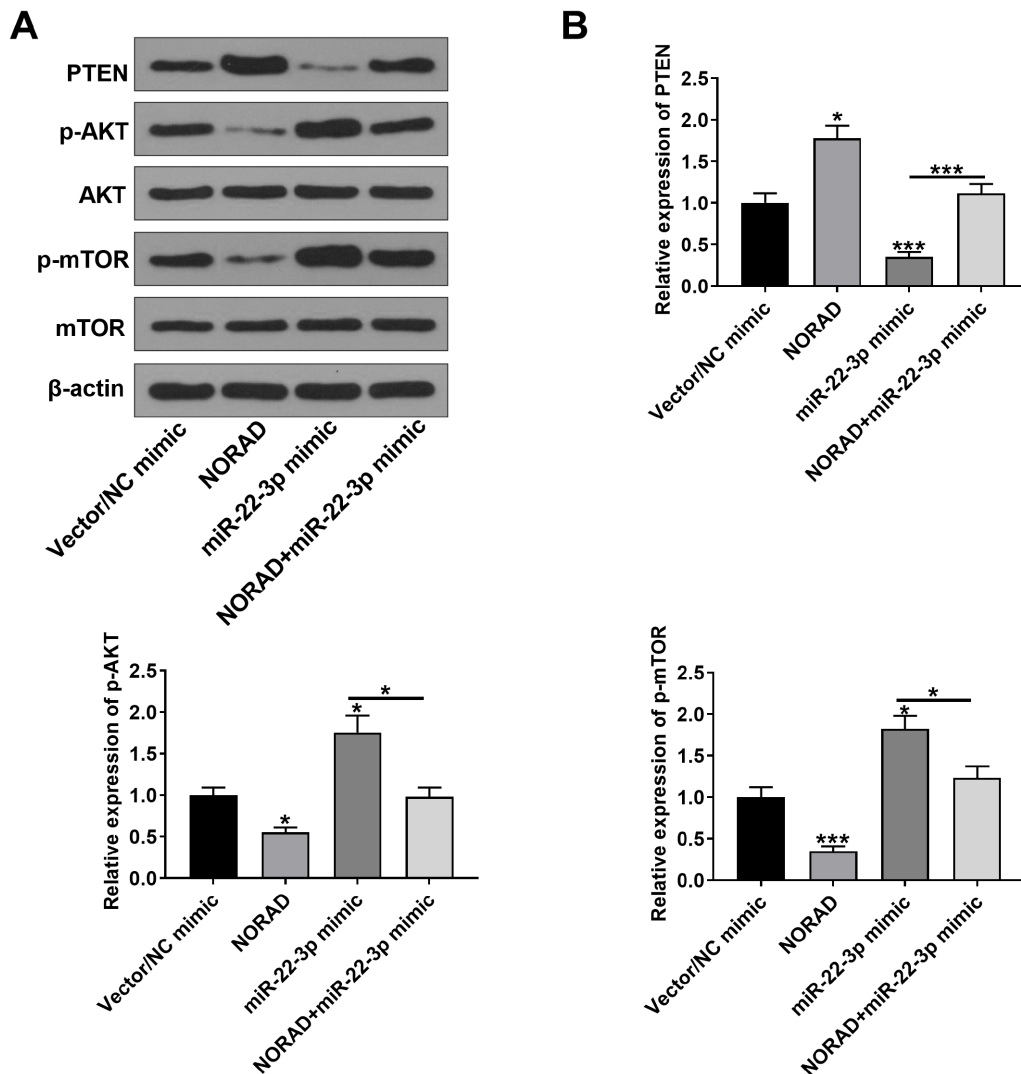


Figure 5. Upregulation of NORAD inhibits the mTOR/AKT signaling pathway by regulating miR-22-3p HL-1 cells were transfected with OE-NORAD, miR-22-3p mimics, or co-transfected with OE-NORAD and miR-22-3p mimics, and then treated with H/R. (A) The protein expressions of PTEN, AKT, p-AKT, mTOR, p-mTOR were evaluated by western blot analysis. (B) Data were analyzed by using the ImageJ2X software. * $P < 0.05$, *** $P < 0.001$.

tion of the mTOR/AKT signaling pathway by sponging miR-22-3p.

Discussion

In the last decades, a large number of lncRNAs have been identified and demonstrated to be closely involved in the progression of AMI, and some of which are considered as potential diagnostic biomarkers or therapeutic targets for AMI. For example, Hu *et al.* [32] found that knockdown of MALAT1 attenuates AMI progression by targeting miR-320, suggesting that MALAT1 might be a potential therapeutic target. Inhibition of Mirt1 efficiently attenuates AMI by suppressing the activation of the NF- κ B signaling [33]. One previous study revealed that downregulation of ANRIL relieves the apoptosis of myocardial cells in AMI by regulating the expression of IL-33/ST2 [34]. Zhuo *et al.* [35] performed an RNA-seq analysis and constructed a lncRNA-miRNA-mRNA network potentially associated with AMI progression, and identified that SNHG8 might be a key regulator of AMI. ZFAS1 was found to act as a SERCA2a inhibitor to cause intracellular Ca²⁺ overloading and contractile dysfunction in a mice model of AMI [36]. Silencing of XIST can significantly repress the apoptosis of myocardial cells in rats with AMI by targeting miR-449 [37]. In addition, many other lncRNAs including Novlnc6, Mhrt, and Tie-1-AS have been shown to play crucial regulatory roles in the development of AMI [38,39]. Although NORAD has been found to be highly expressed in AMI, its function and the molecular mechanisms remain unclear. Here, we confirmed that downregulation of NORAD could efficiently attenuate AMI-induced heart damage in the mice model, suggesting that high expression level of NORAD was positively correlated with AMI progression.

It is well known that lncRNAs can act as competitive endogenous RNAs (ceRNAs) of miRNAs at post-transcriptional level [40,41]. To explore the regulatory mechanism of NORAD in AMI, Starbase v2.0 was used to predict the potential targets of NORAD. We found that there is a putative binding site between NORAD and miR-22-3p.

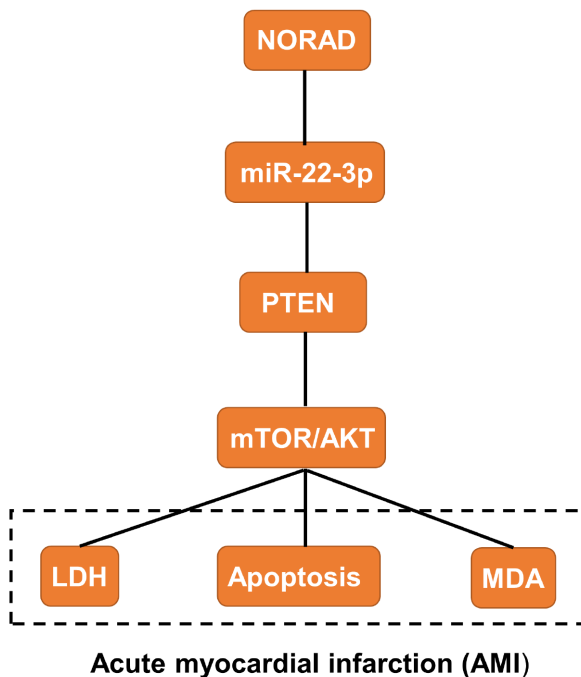


Figure 6. The schematic diagram of proposed mechanism NORAD regulates H/R-induced cardiomyocyte apoptosis and release of LDH and MDA through the miR-22-3p/PTEN axis.

Although the role of miR-22-3p in AMI has not been well studied, miR-22-3p has been identified as a direct target of many lncRNAs and participates in the development of cardiovascular diseases. LncRNA MIAT functions as a ceRNA to upregulate DAPK2 by directly sponging miR-22-3p in diabetic cardiomyopathy [42]. LncRNA H19 has been demonstrated to ameliorate myocardial I/R injury by targeting miR-22-3p [43]. Here, luciferase reporter assay, RNA pull-down assay, and qRT-PCR confirmed that NORAD could sponge miR-22-3p and negatively regulate the expression of miR-22-3p. Moreover, miR-22-3p inhibitor abolished the effects of knockdown of NORAD on the apoptosis and the production of LDH and MDA. These data indicate that the effects of NORAD on AMI are mediated by miR-22-3p.

PTEN has been demonstrated to be closely related to the progression of AMI such as myocardial fibrosis and cardiomyocyte apoptosis, and it always functions as a direct target of miRNAs. For example, Li *et al.* [44] reported that upregulation of miR-23a significantly increases the superoxide dismutase, glutathione and catalase activity levels, and decreases the MDA level in AMI by directly targeting PTEN. MiR-26a regulates myocardial fibrosis after MI by targeting PTEN to modulate the PI3K/AKT signaling pathway [45]. In addition, MiR-214 suppresses left ventricular remodeling in an AMI mice model by inhibiting cellular apoptosis through targeting PTEN, suggesting a positive impact of PTEN on AMI injury [46]. Here, PTEN was identified as a target of miR-22-3p by using Targetscan software, and luciferase reporter assay further determined the binding relationship between miR-22-3p and PTEN. Meanwhile, overexpression of NORAD increased the expression level of PTEN ($P < 0.05$), and miR-22-3p mimics decreased the expression level of PTEN and attenuated the effect of NORAD on the expression of PTEN. Moreover, miR-22-3p mimics inhibited H/R-induced cell apoptosis, while its effect was abolished by overexpression of PTEN. All these data indicate that si-NORAD induces protective effect in AMI *in vitro* by regulating the miR-22-3p/PTEN axis. In addition, PTEN is a well-identified inhibitor of AKT activation and can inactivate the PI3K/AKT/mTOR signaling. It was reported that PTEN affects cardiomyocyte apoptosis through modulation of the mTOR/AKT signaling. Therefore, we explored the effect of NORAD and miR-22-3p on the mTOR/AKT signaling pathway. Our results showed that overexpression of NORAD markedly decreased the expression levels of p-AKT and p-mTOR, while miR-22-3p mimics increased the expression levels of p-AKT and p-mTOR, and attenuated the effects of overexpression of NORAD on the expressions of p-AKT and p-mTOR. These results suggest that NORAD may affect the cardiomyocyte apoptosis and AMI-induced myocardial injury through regulating the mTOR/AKT signaling by targeting the miR-22-3p/PTEN axis (Figure 6). However, whether the manipulation of AKT/mTOR signaling affects the function of NORAD in AMI should be further investigated.

In summary, our study demonstrated that NORAD could promote the progression of MI by targeting the miR-22-3p/PTEN axis, providing a novel therapeutic target for AMI.

Funding

This work was supported by the grant from the Shanxi Science and Technology Commission Innovation Plan (No. 6207022964).

Conflict of Interest

The authors declare that they have no conflict of interest.

References

1. Reed GW, Rossi JE, Cannon CP. Acute myocardial infarction. *Lancet* 2017, 389: 197–210
2. Anderson JL, Morrow DA. Acute myocardial infarction. *N Engl J Med* 2017, 376: 2053–2064
3. Huang L, Guo B, Liu S, Miao C, Li Y. Inhibition of the lncRNA Gpr19 attenuates ischemia-reperfusion injury after acute myocardial infarction by inhibiting apoptosis and oxidative stress via the miR-324-5p/Mtfr1 axis. *IUBMB Life* 2020, 72: 373–383
4. Jiao L, Li M, Shao Y, Zhang Y, Gong M, Yang X, Wang Y, *et al.* lncRNA-ZFAS1 induces mitochondria-mediated apoptosis by causing cytosolic Ca²⁺ overload in myocardial infarction mice model. *Cell Death Dis* 2019, 10: 942
5. Zhou Y, Richards AM, Wang P. MicroRNA-221 is cardioprotective and anti-fibrotic in a rat model of myocardial infarction. *Mol Ther Nucleic Acids* 2019, 17: 185–197
6. Yang C, Wu K, Wang S, Wei G. Long non-coding RNA XIST promotes osteosarcoma progression by targeting YAP via miR-195-5p. *J Cell Biochem* 2018, 119: 5646–5656
7. Alipoor FJ, Asadi MH, Torkzadeh-Mahani M. MIAT lncRNA is overexpressed in breast cancer and its inhibition triggers senescence and G1 arrest in MCF7 cell line. *J Cell Biochem* 2018, 119: 6470–6481
8. Zhao J, Zhang C, Gao Z, Wu H, Gu R, Jiang R. *Retracted*: Long non-coding RNA ASBEL promotes osteosarcoma cell proliferation, migration, and invasion by regulating microRNA-21. *J Cell Biochem* 2018, 119: 6461–6469
9. Wang Z, Jin Y, Ren H, Ma X, Wang B, Wang Y. Downregulation of the long non-coding RNA TUSC7 promotes NSCLC cell proliferation and correlates with poor prognosis. *Am J Transl Res* 2016, 8: 680–687
10. Wu X, Lim ZF, Li Z, Gu L, Ma W, Zhou Q, Su H, *et al.* NORAD expression is associated with adverse prognosis in esophageal squamous cell carcinoma. *Oncol Res Treat* 2017, 40: 370–374
11. Tan BS, Yang MC, Singh S, Chou YC, Chen HY, Wang MY, Wang YC, *et al.* lncRNA NORAD is repressed by the YAP pathway and suppresses lung and breast cancer metastasis by sequestering S100P. *Oncogene* 2019, 38: 5612–5626
12. Li H, Wang X, Wen C, Huo Z, Wang W, Zhan Q, Cheng D, *et al.* Long noncoding RNA NORAD, a novel competing endogenous RNA, enhances the hypoxia-induced epithelial-mesenchymal transition to promote metastasis in pancreatic cancer. *Mol Cancer* 2017, 16: 169
13. He H, Yang H, Liu D, Pei R. lncRNA NORAD promotes thyroid carcinoma progression through targeting miR-202-5p. *Am J Transl Res* 2019, 11: 290–299
14. Yang X, Cai JB, Peng R, Wei CY, Lu JC, Gao C, Shen ZZ, *et al.* The long noncoding RNA NORAD enhances the TGF- β pathway to promote hepatocellular carcinoma progression by targeting miR-202-5p. *J Cell Physiol* 2019, 234: 12051–12060
15. Zhao X, Wei X, Wang X, Qi G. Long non-coding RNA NORAD regulates angiogenesis of human umbilical vein endothelial cells via miR-590-3p under hypoxic conditions. *Mol Med Report* 2020, 21: 2560
16. Xu Y, Cheng M, Mi L, Qiu Y, Hao W, Li L. MiR-22-3p Enhances the chemosensitivity of gastrointestinal stromal tumor cell lines to cisplatin through PTEN/PI3K/Akt pathway. *IJAAI* 2018, 17: 318
17. Ji Q, Wang X, Cai J, Du X, Sun H, Zhang N. MiR-22-3p regulates amyloid β deposit in mice model of Alzheimer's disease by targeting mitogen-activated protein kinase 14. *Curr Neurovasc Res* 2019, 16: 473–480
18. Liu Y, Li H, Liu Y, Zhu Z. MiR-22-3p targeting alpha-enolase 1 regulates the proliferation of retinoblastoma cells. *Biomed Pharmacother* 2018, 105: 805–812
19. Chen J, Wu FX, Luo HL, Liu JJ, Luo T, Bai T, Li LQ, *et al.* Berberine upregulates miR-22-3p to suppress hepatocellular carcinoma cell proliferation by targeting Sp1. *Am J Transl Res* 2016, 8: 4932–4941
20. Zhao XS, Ren Y, Wu Y, Ren HK, Chen H. MiR-30b-5p and miR-22-3p restrain the fibrogenesis of post-myocardial infarction in mice via targeting PTAFR. *Eur Rev Med Pharmacol Sci* 2020, 24: 3993–4004
21. Álvarez-García V, Tawil Y, Wise HM, Leslie NR. Mechanisms of PTEN loss in cancer: It's all about diversity. *Semin Cancer Biol* 2019, 59: 66–79
22. Worby CA, Dixon JE. PTEN. *Annu Rev Biochem* 2014, 83: 641–669
23. Mahmoud AH, Taha NM, Zakhary M, Tadros MS. PTEN gene & TNF-alpha in acute myocardial infarction. *IJC Heart Vasculature* 2019, 23: 100366
24. Mocanu MM, Yellon DM. PTEN, the Achilles' heel of myocardial ischemia/reperfusion injury? *Br J Pharmacol* 2007, 150: 833–838
25. Aoki M, Fujishita T. Oncogenic Roles of the PI3K/AKT/mTOR axis. *Curr Top Microbiol Immunol* 2017, 407: 153–189
26. Sun K, Luo J, Guo J, Yao X, Jing X, Guo F. The PI3K/AKT/mTOR signaling pathway in osteoarthritis: a narrative review. *Osteoarthritis Cartilage* 2020, 28: 400–409
27. Sun XH, Wang X, Zhang Y, Hui J. Exosomes of bone-marrow stromal cells inhibit cardiomyocyte apoptosis under ischemic and hypoxic conditions via miR-486-5p targeting the PTEN/PI3K/AKT signaling pathway. *Thrombosis Res* 2019, 177: 23–32
28. Wu F, Gao F, He S, Jiang Y, Luo G, Xiao Y. c-Jun promotes the survival of H9c2 cells under hypoxia via PTEN/Akt signaling pathway. *J Physiol Biochem* 2019, 75: 433–441
29. Zhao J, Li X, Hu J, Chen F, Qiao S, Sun X, Gao L, *et al.* Mesenchymal stromal cell-derived exosomes attenuate myocardial ischemia-reperfusion injury through miR-182-regulated macrophage polarization. *Cardiovasc Res* 2019, 115: 1205–1216
30. Fan ZG, Qu XL, Chu P, Gao YL, Gao XF, Chen SL, Tian NL. MicroRNA-210 promotes angiogenesis in acute myocardial infarction. *Mol Med Report* 2018, 17: 2658
31. Livak KJ, Schmittgen TD. Analysis of relative gene expression data using real-time quantitative PCR and the 2^{- $\Delta\Delta$ CT} method. *Methods* 2001, 25: 402–408
32. Hu H, Wu J, Li D, Zhou J, Yu H, Ma L. Knockdown of lncRNA MALAT1 attenuates acute myocardial infarction through miR-320-Pten axis. *Biomed Pharmacother* 2018, 106: 738–746
33. Li X, Zhou J, Huang K. Inhibition of the lncRNA Mirt1 attenuates acute myocardial infarction by suppressing NF- κ B activation. *Cell Physiol Biochem* 2017, 42: 1153–1164
34. Yang J, Huang X, Hu F, Fu X, Jiang Z, Chen K. lncRNA ANRIL knock-down relieves myocardial cell apoptosis in acute myocardial infarction by regulating IL-33/ST2. *Cell Cycle* 2019, 18: 3393–3403
35. Zhuo LA, Wen YT, Wang Y, Liang ZF, Wu G, Nong MD, Miao L. lncRNA SNHG8 is identified as a key regulator of acute myocardial infarction by RNA-seq analysis. *Lipids Health Dis* 2019, 18: 201
36. Zhang Y, Jiao L, Sun L, Li Y, Gao Y, Xu C, Shao Y, *et al.* lncRNA ZFAS1 as a SERCA2a inhibitor to cause intracellular Ca²⁺ overload and contractile dysfunction in a mouse model of myocardial infarction. *Circ Res* 2018, 122: 1354–1368
37. Zhang M, Liu HY, Han YL, Wang L, Zhai DD, Ma T, Zhang MJ, *et al.* Silence of lncRNA XIST represses myocardial cell apoptosis in rats with acute myocardial infarction through regulating miR-449. *Eur Rev Med Pharmacol Sci* 2019, 23: 8566–8572
38. Uchida S, Dimmeler S. Long noncoding RNAs in cardiovascular diseases. *Circ Res* 2015, 116: 737–750
39. Guo Y, Luo F, Liu Q, Xu D. Regulatory non-coding RNAs in acute myocardial infarction. *J Cell Mol Med* 2017, 21: 1013–1023

40. Thomson DW, Dinger ME. Endogenous microRNA sponges: evidence and controversy. *Nat Rev Genet* 2016, 17: 272–283
41. Qi X, Zhang DH, Wu N, Xiao JH, Wang X, Ma W. ceRNA in cancer: possible functions and clinical implications. *J Med Genet* 2015, 52: 710–718
42. Zhou X, Zhang W, Jin M, Chen J, Xu W, Kong X. lncRNA MIAT functions as a competing endogenous RNA to upregulate DAPK2 by sponging miR-22-3p in diabetic cardiomyopathy. *Cell Death Dis* 2017, 8: e2929
43. Zhang BF, Chen J, Jiang H. lncRNA H19 ameliorates myocardial ischemia-reperfusion injury by targeting miR-22-3P. *Int J Cardiol* 2019, 278: 224
44. Li S, Ren J, Sun Q. The expression of microRNA-23a regulates acute myocardial infarction in patients and in vitro through targeting PTEN. *Mol Med Report* 2018, 17: 6866
45. Zhang S, Cui R. The targeted regulation of miR-26a on PTEN-PI3K/AKT signaling pathway in myocardial fibrosis after myocardial infarction. *Eur Rev Med Pharmacol Sci* 2018, 22: 523–531
46. Yang X, Qin Y, Shao S, Yu Y, Zhang C, Dong H, Lv G, *et al.* MicroRNA-214 inhibits left ventricular remodeling in an acute myocardial infarction rat model by suppressing cellular apoptosis via the phosphatase and tensin homolog (PTEN). *Int Heart J* 2016, 57: 247–250